Water-Soluble Interpolyelectrolyte Complexes of Polyisobutylene-*block*-Poly(methacrylic acid) Micelles: Formation and Properties

Markus Burkhardt,[†] Markus Ruppel,[†] Sandrine Tea,[†] Markus Drechsler,[†] Ralf Schweins,[‡] Dmitry V. Pergushov,[§] Michael Gradzielski,[£] Alexander B. Zezin,[§] and Axel H. E. Müller*[,†]

Makromolekulare Chemie II, Universitä t Bayreuth, D-95440 Bayreuth, Germany, Institut Laue-Langevin, 38042 Grenoble Cedex 9, France, Department of Polymer Science, School of Chemistry, Moscow State University, 119991 Moscow, Russia, and Stranski Laboratorium für Physikalische und Theoretische Chemie, Institut für Chemie, Technische Universität Berlin, D-10623 Berlin, Germany

Received June 21, 2007. In Final Form: November 27, 2007

We report on interpolyelectrolyte complexes (IPECs) formed by micelles of ionic amphiphilic diblock copolymers with polyisobutylene (PIB) and poly(sodium methacrylate) (PMANa) blocks interacting with quaternized poly(4-vinylpyridine) (P4VPQ). The interpolyelectrolyte complexation was followed by turbidimetry and small angle neutron scattering (SANS). The data obtained by means of a combination of SANS, dynamic light scattering (DLS), and cryogenic transmission electron microscopy (cryo-TEM) provide evidence on the core−shell−corona structure of the complex species with the shell assembled from fragments of electrostatically bound PMANa and quaternized P4VPQ fragments, original PIB_x-*b*-$PMAA_y$ micelles apparently playing a lyophilizing part. The complex formation is followed by potentiometric titration as well. This process is initially kinetically controlled. In the second step larger aggregates rearrange in favor of smaller complexes with core−shell−corona structure, which are thermodynamically more stable. An increase in ionic strength of the solution results in dissociation of the complex species as proven by SANS and analytical ultracentrifugation (AUC). This process begins at the certain threshold ionic strength and proceeds via a salt-induced gradual release of chains of the cationic polyectrolyte from the complex species.

1. Introduction

Ionic amphiphilic diblock copolymers are of considerable importance due to their numerous[1] possible promising applications in various fields, including industry, ecology, biotechnology, and medicine. Their properties, in particular their self-assembly behavior in selective solvents, leading to the formation of macromolecular micelles, resemble those manifested by common low-molecular-weight surfactants, though the formed polymeric micelles are considerably less responsive, i.e., the influence of variations of external conditions (pH, ionic strength, etc.) on their aggregation numbers is much less pronounced than for low-molecular-weight surfactant systems. A presence of a polyelectrolyte block in such copolymers provides a unique possibility to tune the characteristics of the formed macromolecular assemblies (e.g., their size, shape, and in some cases even aggregation number) via a simple variation of conditions of the surrounding solution (e.g., pH or ionic strength). Besides, the ionic amphiphilic diblock copolymers can obviously interact with oppositely charged molecules.

Several attempts have been reported to obtain polyelectrolyte complexes (PECs) of homopolymers with oppositely charged surfactants.[2,3] Babak et al. reported on chitosan capsules stabilized by a shell formed by an electrostatic complex. The complex is formed by chitosan as a semirigid positively charged polyelectrolyte and sodium dodecyl sulfate (SDS) as anionic surfactant. They report that the cationic polymer chains are cross-linked by a shell consisting of a network containing anionic surfactant micelles.

Special architectures like brushes were investigated as well.[4] Complexes with enzymes[5] or DNA[6] and their possible applications as carriers were also reported.[7] Another attempt, offering a novel route for a design of yet unexplored complex macromolecular architectures stabilized by interpolymer salt bonds, is the complexation of oppositely charged macromolecules. Such complex macromolecular assemblies are traditionally related to so-called interpolyelectrolyte complexes (IPECs).

The domain of IPECs has been very extensively investigated by a number of research groups during the past decades. The results of those studies have been exhaustively reviewed elsewhere,[2,8,9] with the main attention devoted to the complex macromolecular architectures based on the oppositely charged linear homopolyelectrolytes. The structure and properties of IPECs are determined by a number of factors: the characteristics of the polymeric components (e.g., nature of their ionic groups, degrees of polymerization, charge density, etc.) and their concentrations, the ratio between amounts of the oppositely charged groups of polyelectrolytes, the conditions of the surrounding solution (e.g., ionic strength, degree of neutralization (α), pH, temperature, etc.), and in some cases the method of the

* To whom correspondence should be addressed. E-mail: axel.mueller@uni-bayreuth.de.

[†] Universität Bayreuth.

[‡] Institut Laue-Langevin.

[§] Moscow State University.

[£] Technische Universität Berlin.

(1) Förster, S.; Abetz, V.; Müller, A. H. E. *Adv. Polym. Sci.* **2004**, *166*, 173.

(2) Thünemann, A. F.; Müller, M.; Dautzenberg, H.; Joanny, J.-F.; Löwen, H. *Adv. Pol. Sci.* **2004**, *166*, 113.

(3) Babak, V. G.; Merkovich, E. A.; Desbrieres, J.; Rinaudo, M. *Pol. Bull.* **2000**, *45*, 77.

(4) Konradi, R.; Rühe, J. *Macromolecules* **2005**, *38*, 6140.

(5) Matsudo, T.; Ogawa, K.; Kokufuta, E. *Biomacromolecules* **2003**, *4*, 1794.

(6) Gossl, I.; Shu, L.; Schlüter, A. D.; Rabe, J. P. *J. Am. Chem. Soc.* **2002**, *124*, 6860.

(7) Sonoda, T.; Niidome, T.; Katayama, Y. *Recent Res. Dev. Bioconj. Chem.* **2005**, *2*, 145.

(8) Smid, J.; Fish, D.; In: Mark, H. F.; Bikales, N. M.; Overberger, C. G.; Menges, G. *Encyclopedia of polymer science and engineering*; Wiley: New York, 1988; Vol. 11, p 720.

(9) Philipp, B.; Dautzenberg, H.; Linow, K.-J.; Koetz, J.; Dawydoff, W. *Prog. Polym. Sci.* **1989**, *14*, 91.

10.1021/la701835r CCC: $40.75
Published on Web 01/29/2008

preparation of such complex macromolecular assemblies. The use of ionic diblock copolymers, including ionic amphiphilic diblock copolymers self-assembling in aqueous media with the formation of macromolecular micelles, as polymeric components in interpolyelectrolyte complexation provides an attractive opportunity to design novel complex macromolecular architectures of micellar type,[10−22] which are thought to be utilized as stimuli-responsive nanocarriers or nanoreactors.

In our previous papers,[20−22] we have demonstrated that polyisobutylene-*b*-poly(sodium methacrylate) (PIB_x-*b*-$PMANa_y$) micelles interacting with a linear cationic polyelectrolyte, viz. poly(*N*-ethyl-4-vinylpyridinium bromide) (P4VPQ), can form complex species in which the original PIB_x-*b*-$PMANa_y$ micelles apparently play a lyophilizing part. The diblock copolymers were synthesized via combination of cationic polymerization of isobutylene followed by transfer to anionic polymerization to polymerize the second block, poly(*tert*-butyl methacrylate) (P*t*BMA), as reported by Martinez-Castro et al.[23] Thus, such novel complex macromolecular architectures represent a kind of polymeric hybrids combining features of the macromolecular micelles with those typical for the common IPECs. The experimental results obtained by a combination of various techniques (SANS, flourescence spectroscopy (FS), DLS) have provided conclusive evidence on a peculiar core−shell−corona ("onionlike") structure of the formed complex species, with a core formed by PIB blocks, a shell assembled from the coupled oppositely charged polyelectrolyte fragments, and a corona built up from the fragments of PMANa blocks not involved in interpolyelectrolyte complexation, the aggregation number of the original PIB_x-*b*-$PMANa_y$ micelles appearing to remain nearly constant upon the interpolyelectrolyte complexation. Later, a similar core−shell−corona structure has been also suggested for the complex species derived from polystyrene-*b*-poly(*N*-ethyl-4-vinylpyridinium bromide) (PS-*b*-P4VPQ) micelles interacting with a linear anionic polyelectrolyte, viz. poly(sodium methacrylate) (PMANa).[24]

This paper considerably extends our previous investigations on IPECs based on the PIB_x-*b*-$PMANa_y$ micelles, showing that the proposed core−shell−corona structure exists for a number of copolymers with different lengths of their blocks. Besides, we demonstrate that interpolyelectrolyte complexation apparently does not render the PIB_x-*b*-$PMANa_y$ micelles from "dynamic" (as thoroughly discussed in[25]) to "frozen" ones: the number of the PIB_x-*b*-$PMANa_y$ molecules incorporated into the complex species changes upon the variation of conditions of the surrounding solution (e.g., pH). In addition, we have examined salt-induced dissociation of such complex macromolecular architectures.

Table 1. Molecular Characteristics of the Polymers Used in This Work

polymer	DP_n, PIB	DP_n, PtBMA	PDI (GPC)	M_n (calcd) (g/mol)
1[a]	20	100	1.16	9620
2[a]	20	280	1.10	24 920
3[a]	20	425	1.20	37 250
4	25	350	1.22	31 600
5	30	190	1.14	18 000
6	30	170	1.12	16 400
7	75	190	1.09	20 500
8	75	615	1.05	57 000
9	75	1600	1.03	141 000

[a] These polymers were synthesized via a different route.[26]

2. Experimental Section

2.1. Materials. Polyisobutylene-*b*-poly(*tert*-butyl methacrylate) diblock copolymers (PIB-*b*-P*t*BMA) were synthesized via combination of living cationic and anionic polymerizations as described elsewhere.[23,26] Size exclusion chromatography (SEC) was used to determine the molecular weight distributions of the PIB precursor (measured separately) and PIB-*b*-P*t*BMA using PIB and P*t*BMA standards. For the diblock copolymer, a weighted average of the homopolymer calibration curve was used. SEC was performed using PSS SDV-gel columns (5 μm, 60 cm, 1 × linear (10^2−10^5 Å), 1 × 100 Å) with THF as eluent at a flow rate of 1.0 mL/min at room temperature using UV (λ = 230 and 260 nm) and RI detection. The values of the number-average degree of polymerization, DP_n, of the blocks and the calculated number-average molecular masses, $\overline{M_n}$, for the corresponding hydrolyzed diblock copolymers PIB-*b*-PMAA are shown in Table 1. The values were calculated from the values of M_n for the corresponding values of M_n PIB-*b*-P*t*BMA diblock copolymers measured by means of SEC. The polydispersity indices of PIB-*b*-P*t*BMA are in the range of 1.03−1.22. After hydrolysis of the block copolymer with hydrochloric acid in dioxane at 80 °C for 24 h polyisobutylene-*b*-poly(methacrylic acid) (PIB-*b*-PMAA) copolymer was obtained.

P4VPQ was synthesized from poly(4-vinylpyridine) with weight-average molar mass M_w = 60 000 g/mol (Aldrich, DP_w = 600) and M_w = 50 000 g/mol (Polysciences Inc., DP_w = 500) via its exhaustive quaternization with a 10-fold excess of ethyl bromide at 60 °C in methanol. As determined by ^{1}H NMR spectroscopy, the molar fraction of quaternized pyridine units in the resulting polymer was close to 0.9, corresponding to about 540 and 450 charged monomer units per polymer chain, respectively.

2.2. Sample Preparation. To prepare a stock solution of the copolymer, PIB_x-*b*-$PMAA_y$, NaCl (Merck) and TRIS buffer (2-amino-2-(hydroxymethyl)-1,3-propanediol, Fluka) were dissolved in NaOH solutions at room temperature (RT) under continuous stirring for at least 24 h. The amount of NaOH was calculated according to the number of COOH groups of the weighed polymer. The solutions all showed low viscosity and were transparent.

For preparation of the complexes, a stock solution of the P4VPQ was prepared, dissolving a calculated amount of P4VPQ in Milli-Q water (resistance = 18 MΩ) containing NaCl and 0.01 M TRIS. The polymer dissolved immediately. The calculated amount of P4VPQ solution was added to the solution containing the micelles under vigorous stirring, until a slight turbidity could be seen. The solution

(10) Harada, A.; Kataoka, K. *Macromolecules* **1995**, *28*, 5294.
(11) Kataoka, K.; Togawa, H.; Harada, A.; Yasugi, K.; Matsumoto, T.; Katayose, S. *Macromolecules* **1996**, *29*, 8556.
(12) Kabanov, A. V.; Bronich, T. K.; Kabanov, V. A.; Yu, K.; Eisenberg, A. *Macromolecules* **1996**, *29*, 288.
(13) Harada, A.; Kataoka, K. *Macromolecules* **1998**, *31*, 6140.
(14) Cohen Stuart, M. A.; Besseling, N. A. M.; Fokkink, R. G. *Langmuir* **1998**, *14*, 6846.
(15) Harada, A.; Kataoka, K. *Langmuir* **1999**, *15*, 4208.
(16) Bronich, T. K.; Nguen, H. K.; Eisenberg, A.; Kabanov, A. V. *J. Am. Chem. Soc.* **2000**, *122*, 8339.
(17) Gohy, J.-F.; Varshney, S. K.; Antoun, S.; Jerome, R. *Macromolecules* **2000**, *33*, 9298.
(18) Talingting, M. R.; Voigt, U.; Munk, P.; Webber, S. E. *Macromolecules* **2000**, *33*, 9612.
(19) Gohy, J.-F.; Varshney, S. K.; Jerome, R. *Macromolecules* **2001**, *34*, 2745.
(20) Pergushov, D. V.; Remizova, E. V.; Feldthusen, J.; Zezin, A. B.; Müller, A. H. E.; Kabanov, V. A.; *J. Phys. Chem. B* **2003**, *107*, 8093.
(21) Pergushov, D. V.; Remizova, E. V.; Feldthusen, J.; Gradzielski, M.; Lindner, P.; Zezin, A. B.; Müller, A. H. E.; Kabanov, V. A. *Polymer* **2004**, *45*, 367.
(22) Pergushov, D. V.; Gradzielski, M.; Burkhardt, M.; Remizova, E. V.; Zezin, A. B.; Kabanov, V. A.; Müller, A. H. E. *Pol. Prepr.* **2004**, *45*, 236.
(23) Martinez-Castro, N.; Lanzendörfer, M. G.; Müller, A. H. E.; Cho, J. C.; Acar, M. H.; Faust, R. *Macromolecules* **2003**, *36*, 6985.
(24) Lysenko, E. A.; Chelushkin, P. S.; Bronich, T. K.; Eisenberg, A.; Kabanov, V. A.; Kabanov, A. V. *J. Phys. Chem. B* **2004**, *108*, 12352.
(25) Burkhardt, M.; Martinez-Castro, N.; Tea, S.; Drechsler, M.; Babin, I.; Grishagin, I.; Schweins, R.; Pergushov, D. V.; Gradzielski, M.; Zezin, A. B.; Müller, A. H. E. *Langmuir* **2007**, *23*, 12864.
(26) Feldthusen, J.; Ivan, B.; Müller, A. H. E. *Macromolecules* **1998**, *31*, 578.

was stirred until the solution was completely transparent again. Then, more polycation solution was added to the complexes until the desired value of Z was achieved, where Z is the ratio of the molar concentrations of ionic groups of the oppositely charged polymeric components, Z = [P4VPQ]/[PIB-*b*-PMANa].

2.3. Methods. *2.3.1. Potentiometric Titrations.* Potentiometric and turbitity titrations were conducted in aqueous solutions of the polymers employing a computer-controlled titrator (Titrando 806, Metrohm). Potentiometric sodium ion selective measurements were performed with a Na^+-selective polymer membrane electrode (6.0508.100, METROHM). Turbidity was monitored with a photometer (Spectrosense 523 nm, 6.1109.110, Metrohm). For complexation, a calculated amount of P4VPQ solution was added to the micellar solution applying the highest dosing rate (16 mL/min). The turbidity was monitored until a plateau was reached. Then, further portions of the solution of P4VPQ were added to obtain complexes with higher Z values.

2.3.2. Cryogenic Transmission Electron Microscopy (Cryo-TEM).[27] Samples were prepared as described above. The polymers were dissolved in aqueous solutions of CsOH (Fluka). To achieve the desired ionic strength, CsCl (Acros) was used. For cryo-TEM studies, a drop of the sample was placed on an untreated bare copper transmission electron microscopy (TEM) grid (600 mesh, Science Services, München, Germany). Most of the liquid was removed with blotting paper, leaving a thin film stretched over the grid holes. The specimens were shock-vitrified by rapid immersion into liquid ethane and cooled to ~90 K by liquid nitrogen in a temperature-controlled freezing unit (Zeiss Cryobox, Zeiss NTS GmbH, Oberkochen, Germany). The temperature was monitored and kept constant in the chamber during all of the sample preparation steps. After freezing the specimens, the remaining ethane was removed using blotting paper. The specimen was inserted into a cryo-transfer holder (CT3500, Gatan, München, Germany) and transferred to a Zeiss EM922 EF-TEM instrument. Examinations were carried out at temperatures around 90 K. The transmission electron microscope was operated at an acceleration voltage of 200 kV. Zero-loss filtered images (ΔE = 0 eV) were taken under reduced dose conditions (100−1000 e/nm^2). All images were registered digitally by a bottom-mounted CCD camera system (Ultrascan 1000, Gatan) combined and processed with a digital imaging processing system (Gatan Digital Micrograph 3.9 for GMS 1.4).

2.3.3. Dynamic Light Scattering (DLS). Sample solutions for DLS experiments were obtained by an isoionic 50-fold dilution of the sample solutions prepared for the SANS measurements (1 wt %, see Section 2.3.4 below) with corresponding aqueous H_2O solutions of NaCl. The prepared sample solutions were thoroughly filtered by passing at least three times through a Nylon filter (13-HV, Millipore) with a pore size of 0.45 μm. In addition, samples were also prepared as described above with an amount of polymer of about c_{Pol} = 0.02 wt %. The DLS measurements were carried out in sealed cylindrical scattering cells (d = 10 mm) at five scattering angles 30°, 60°, 90°, 120°, and 150° with the use of an ALV DLS/SLS-SP 5022F equipment consisting of an ALV-SP 125 laser goniometer, an ALV 5000/E correlator (cross correlation), and a He−Ne laser with the wavelength λ = 632.8 nm. The CONTIN algorithm was applied to analyze the obtained correlation functions. Apparent hydrodynamic radii, R_h, of the macromolecular assemblies were calculated according to the Stokes−Einstein equation.

2.3.4. Small Angle Neutron Scattering (SANS).[28,29] Sample solutions for SANS experiments were prepared by dissolving PIB$_x$-*b*-PMAA$_y$ in D_2O (Aldrich), containing a desired amount of NaOH (Riedel-de Haën), at RT under continuous stirring overnight. P4VPQ was dissolved in D_2O. The complexes were prepared as described above. The final concentration of the complex in the sample solutions was ca. 1.0 wt %. In all cases, the prepared solutions were homogeneous, transparent, partially colored (slightly brownish), and of low viscosity.

The sample solutions were filled into quartz cells with 2 mm path length (Hellma). In the case of samples at pH 10, the pH value was controlled upon addition of 0.01 M of TRIS buffer (Merck) to the sample solutions. The ionic strength of the sample solutions was adjusted by adding NaCl (Merck). The SANS measurements were performed using the instrument D11 of the Institute Max von Laue-Paul Langevin (ILL, Grenoble, France) with a neutron wavelength λ = 6 Å. Sample-to-detector distances of 1.1, 4, and 16 m were employed. With these configurations, a total range of the magnitude of the scattering vector, q = 0.003−0.35 Å, was covered. The detector sensitivity and the intensity of the primary beam were calibrated by a comparison with the scattering from a 1 mm reference sample of water. The obtained data were radially averaged and corrected for the detector background, the detector dead time, and the scattering from an empty cell. They then were converted into absolute units by a comparison with the scattering from water according to standard routines supplied by the ILL[30] using the GRASP software. It should be noted that the SANS curves presented in this paper still contain the incoherent background scattering of the solvent and the sample.

2.3.5. Analytical Ultracentrifugation (AUC). Sample solutions were obtained by mixing the stock solutions of PIB$_{20}$-*b*-PMAA$_y$ and P4VPQ in the presence of the desired amount of NaCl, followed by a subsequent dilution of such mixtures with 0.01 M TRIS. The sedimentation experiments were carried out with a Beckman (Spinco, Model E) analytical ultracentrifuge equipped with a UV−vis absorption optical detector (Scan mode). The speed of rotor rotation was 48 000 rpm.

3. Results and Discussion

3.1. Complexation. *3.1.1. Turbidimetric Titrations.* Turbidimetric titrations allow an insight into the complexation phenomenon, as the turbidity of a solution is strongly related to the scattering properties and with this to the mass and size of the particles comprised. Even visually decreased transmittance (corresponding to increased turbidity) could be observed during complexation of the micellar solutions with addition of P4VPQ. The transmittance of the complex solution increased with time of stirring. Hence, quantitative turbidimetric measurements were carried out. A certain amount of P4VPQ (V = 1.2 mL, $c \approx$ 2 g/L) was added isoionically (c_{NaCl} = 0.1 M) at the constant value of pH 9) within $t \approx$ 5 s to a micellar solution of PIB$_{75}$-*b*-PMAA$_{1600}$ (V = 10 mL, $c \approx$ 2 g/L) to obtain Z = 0.4. The polycation solution was added with highest rate of addition to enable fast mixing under vigorous stirring. As the addition of the polycation was started manually, the first few seconds of the measurement were taken as a background (Figure 1). Immediately after the start of the addition, a pronounced increase in turbidity could be observed.

After the minimum in transmittance was reached at about T = 0.05, an increase in transmittance could be observed, reaching a plateau at T = 0.57 after 120 min.

The observed increase of turbidity (decrease in transmittance) on addition of P4VPQ into an aqueous solution of PIB$_{75}$-*b*-PMAA$_{1600}$ micelles (Figure 1, the first drop) points to generation of large species with considerably larger mass (and size) compared to the pure micelles, shown as a sketch in Figure 2 (Step 1). They might be formed as nonequilibrium structures due to nonideal mixing resulting in the formation of multimicellar aggregates comprising PIB$_{75}$-*b*-PMAA$_{1600}$ micelles bound each other through macromolecules of the cationic polyelectrolyte.

The following increase in transmittance (decrease in turbidity) reaching a plateau value of T = 0.55 after 10 min indicates that

(27) Adrian, M.; Dubochet, J.; Lepault, J.; McDowall, A. W. *Nature* **1984**, *308*, 32.
(28) Jacrot, B.; Zacchai, G. *Biopolymers* **1981**, *20*, 2413.
(29) Chen, S.-H.; Lin, T.-L. *Methods of Experimental Physics*; Academic Press: New York, 1987; p 489.
(30) GRAS$_{ans}$P; Charles Dewhurst; email: dewhurst@ill.fr; Institut Laue Langevin, Grenoble, France.

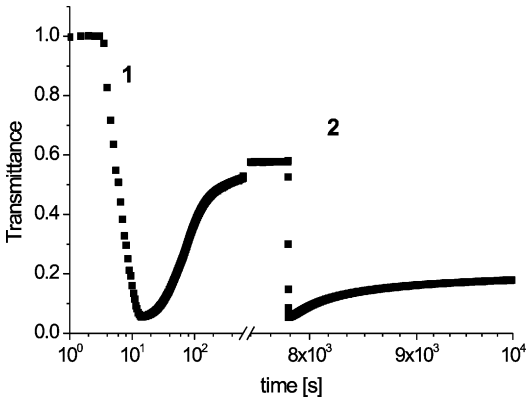

Figure 1. Turbidimetric measurement of the complexation of PIB_{75}-*b*-$PMAA_{1600}$ with addition of P4VPQ to obtain $Z = 0.4$ (1) and 0.5 (2) at $c_{TRIS} = 0.01$ M, $c_{NaCl} = 0.1$ M.

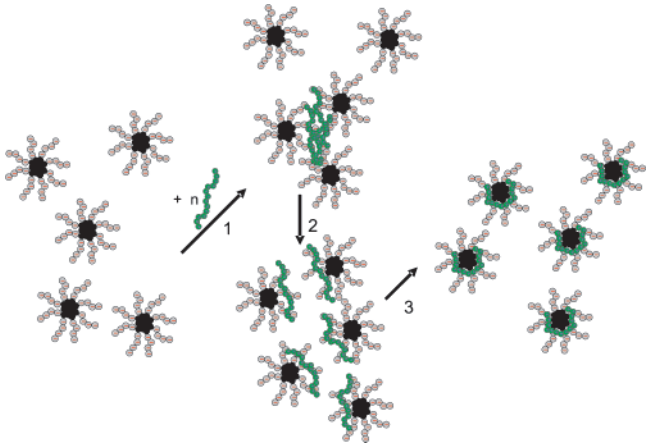

Figure 2. Proposed mechanism of formation of IPECs of spherical negatively charged polyelectrolyte micelles with cationic polyelectrolyte. The use of five micelles is just arbitrarily and should just represent a part of the solution. The polycation added is also not represented quantitatively.

the formed large species become smaller. This effect can be explained by disaggregation of these large species proceeding via so-called polyion exchange reactions, that is, these multimicellar aggregates interacting with free PIB_{75}-*b*-$PMAA_{1600}$ micelles present in the solution in an excess gradually split into smaller aggregates (Figure 2, Step 2). Such a rearrangement finally leading to the formation of equilibrium complex species from nonequilibrium large aggregates generated right away upon mixing aqueous solutions of the oppositely charged linear polyelectrolytes was previously described by Bakeev et al.[31]

At the same time, chains of P4VPQ bound at first to peripheral (outmost) parts of micellar corona of each PIB_{75}-*b*-$PMAA_{1600}$ micelle are assumed then to penetrate deeper inside to be eventually located at the core−corona interface (Figure 2, Step 3). The reason for that is the hydrophobic nature of the product of the interpolyelectrolyte complexation because of the charge neutralization. This favors the minimization of the interface toward the aqueous phase. This results in increasing negative charge of the peripheral (outmost) parts of micellar coronas, leading, in turn, to separation of complex assemblies due to electrostatic repulsion and providing their stability in aqueous media.

To further complex the remaining charges up to $Z = 0.5$, another 0.3 mL of polycation was added, leading to a second decrease in transmittance down to $T = 0.05$. This mixture was

(31) Bakeev, K. N.; Izumrudov, V. A.; Kuchanov, S. I; Zezin, A. B.; Kabanov, V. A. *Macromolecules* **1992**, *25*, 4249.

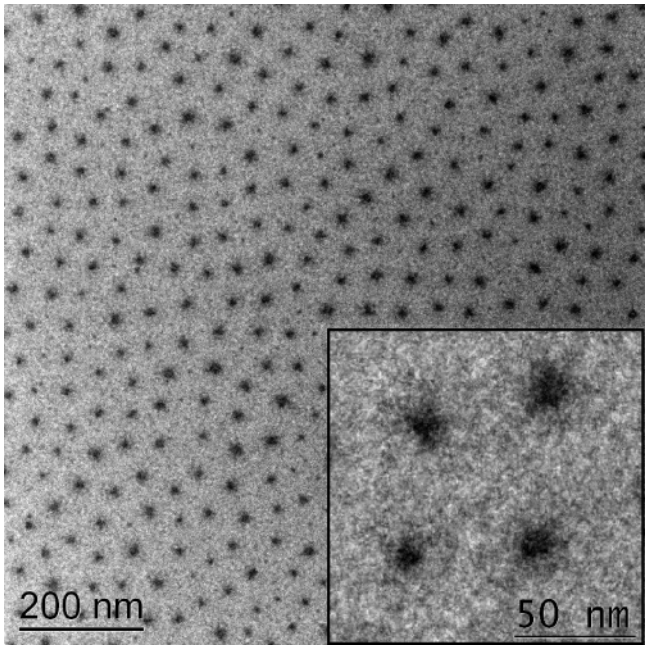

Figure 3. Cryo-TEM image of PIB_{30}-*b*-$PMACs_{170}$, $c_{CsCl} = 0.1$ M, CsOH, $\alpha = 1$, $c_{Pol} = 0.5$ wt %.

also stirred to let the complexes relax to obtain equilibrium structures. This time a plateau value of $T = 0.18$ was reached after 30 min. After addition of the second amount of P4VPQ, a further increase in turbidity can be observed. Here also a complexation and formation of assemblies of complexes followed by rearrangement and decrease of size afterward can be stated. This shows that there are still vacant sites in the corona that can be complexed with the polycation. The increase of transmittance with time is not that pronounced as after addition of the first portion of P4VPQ, showing that there are larger aggregates after reaching the plateau compared to the aggregates after addition of the first portion of P4VPQ. It is remarkable that no precipitation was observed even at $Z = 0.5$. However, the size of the micellar complexes is comparable to the size of the precursor micelles as shown below by means of DLS. In this case, lower transmittance (or higher turbidity) means that the aggregates with larger inner dense nuclei (PIB core + complex shell) are generated.

3.1.2. Cryo-TEM. For all investigations, complexes were formed as described in the Experimental Section. The complex solutions were still transparent. It has to be pointed out that CsOH and CsCl were added to stain PMAA blocks, forming coronae of the PIB-*b*-PMAA micelles, making them visible. Though the affinity of Cs^+ to PMAA is known to be lower than the affinity of Na^+ to PMAA, the results discussed in this paper do not change on the qualitative level.

Cryo-TEM images show micelles (Figure 3) and complexes (Figure 4), respectively. The micelles consist of a dark core, containing the water-insoluble PIB.[25] The surrounding slightly dark shade comprises denser parts of the corona consisting of PMACs, resulting in better electron contrast. The larger the distance of the PMACs from the core, the less dense the corona is and the brighter the region appears in cryo-TEM images. The outer parts of the micelle disappear in the background scattering of the solvent, i.e., water and remaining Cs^+ and Cl^- ions. The same can be seen in the case of the complexes (Figure 4). The core is surrounded by a corona of decreasing darkness. It was proposed by Pergushov et al. that the complexes in the equilibrium state possess a core−shell−corona structure.[20,21] With cryo-TEM this cannot be demonstrated directly because the contrast (i.e.,

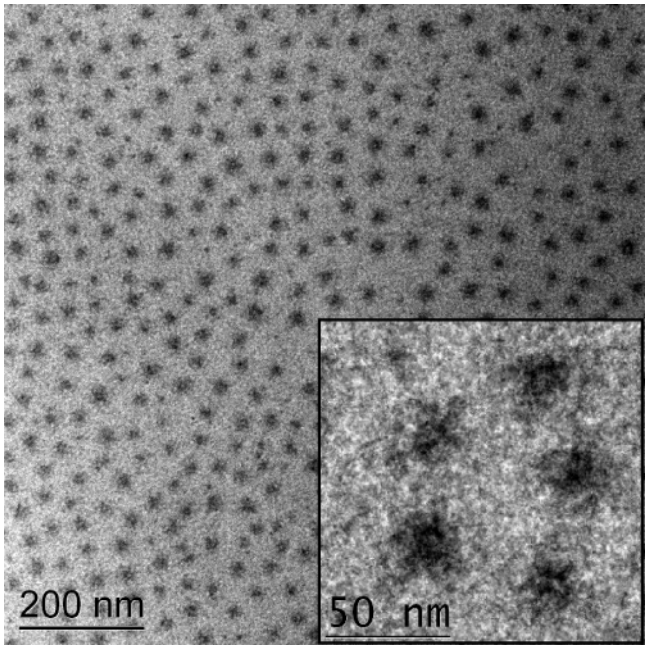

Figure 4. Cryo-TEM image of complex of P4VPQ with PIB_{30}-*b*-$PMACs_{170}$ at $Z = 0.4$, $c_{CsCl} = 0.1$ M, CsOH, $\alpha = 1$, $c_{Pol} = 0.5$ wt %.

electron density) between the complex, core, and the CsCl solution is too low. Additionally, the scattering noise is overlaying the small differences in scattering power. By increasing the intensity of the electron beam to have a better signal-to-noise (S/N) ratio, the sample, especially the PIB core, is immediately destroyed by radiation damage.

If a polycation was complexed in the corona of the micelle, a darker spot in the vicinity of the core should be seen. As no small dark spots in the corona region of the complexes can be found, this is in good agreement with the proposed core−shell−corona structure of such IPECs. Since the charge-neutral complex is hydrophobic, it is trying to decrease the interfacial area toward water. This happens by penetrating the corona of the micellar aggregate and wrapping around the hydrophobic PIB. So the energetically favored region where the complex is situated should be in the vicinity of the core.

The particles are still separated, showing no further aggregation or formation of superstructures. Thus, P4VPQ does not link several micelles, resulting in generation of large aggregates. The narrow size distribution shown in the micrograph supports the equilibrium state of the complexes as well. In the case of a nonequilibrium state, larger aggregates of several micelles cross-linked with one P4VPQ chain, resulting in high polydispersity in size, should be observed.

Comparing the cryo-TEM images for the complex and the precursor micelle, some differences can be seen. It has to be emphasized, that the imaging conditions for both images were the same. In the overview, the particles present in the image for complexes are arranged more densely than in the image for the pure micelles. After addition of P4VPQ to the solution of PIB-*b*-PMACs micelles, extended PMACs blocks undergo a certain shrinkage because of charge neutralization.

In the insets of Figures 3 and 4, some of the micelles are zoomed. With respect to the darker areas of the inset (hydrophobic parts of the micellar assemblies), slight changes can be observed. For the pure micelles, the dark part is more compact and the change in scattering contrast is well defined. However, the hydrophobic part of the complex micelles is less defined and the contrast boundaries are smoother. This is assumed to be due to

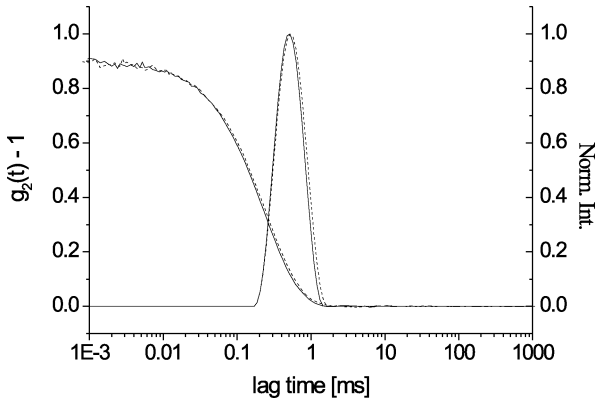

Figure 5. Intensity autocorrelation function and CONTIN plot of micellar solution (dashed) and IPEC with P4VPQ at $Z = 0.4$ (solid) of PIB_{30}-*b*-$PMANa_{170}$, $c_{TRIS} = 0.01$M, $\alpha = 1$ with $c_{NaCl} = 0.1$ M, $\Theta = 90°$.

Table 2. Apparent Hydrodynamic Radii (R_h) of PIB_x-*b*-$PMANa_y$ Micelles and Their IPECs Prepared at $Z = 0.4$, Scattering Angle $\Theta = 90°$, RT, $c_{NaCl} = 0.1$ M, $c_{TRIS} = 0.01$ M Obtained from DLS Measurements at $\alpha = 1$

$\overline{DP_n}$, PIB	$\overline{DP_n}$, PMANa	R_h, micelle [nm]	R_h, IPEC [nm]	R_{IPEC}/R_{Mic}
20	100	22.5	19	0.80
20	280	37	29	0.78
20	425	46.5	33	0.71
30	170	40	38	0.95
30	190	41	39	0.95
75	190	42	40	0.95
75	615	88	71	0.81
75	1600	101.5	81	0.79

the P4VPQ-PMAA complex present in the vicinity of the PIB core. The electron density of the complex is higher than the one of the pure PMACs chains. Hence, they appear as a darker region in the cryo-TEM image. Compared to the PIB core, they are less dense. Thus, the complex worsens the contrast between the hydrophobic part and the background.

3.1.3. Dynamic Light Scattering. DLS measurements provide apparent hydrodynamic radii, R_h, of the micellar assemblies. The distribution of the complexed particle sizes is monomodal (Figure 5). Compared to the pure micellar solutions of PIB_x-*b*-$PMAA_y$ diblock copolymer, the R_h appears to be slightly smaller, as seen from a shift of the decay curve to shorter times. It has to be pointed out that all samples prepared for DLS were measured several days after the preparation to avoid any effects related to the kinetically driven formation of larger aggregates at the early stage of complex preparation.

In Table 2 values for $R_{h,IPEC}/R_{h,Micelle}$ deduced from apparent hydrodynamic radii from DLS measurements are given. They show that the hydrodynamic radii of the micellar assemblies decrease but not significantly compared to those of the precursor micelles (not more than for 20%). The obvious reason for this is complexation of the PMANa chains with P4VPQ leading to a decrease of the number of free negative charges and, therefore, to an effective shortening of the PMANa arms due to the fact that 40% of it are compacted into the complex shell. Hence, they can arrange in a denser way, resulting to less extented micellar corona.

3.1.4. SANS. SANS measurements are also suited to follow the complexation of PIB_x-*b*-$PMAA_y$ with P4VPQ. The increase of M_w of the micelle due to complex formation results in higher scattering intensity at low q values (Guinier region).

In Figure 6 the micellar and complexed state of PIB_{75}-*b*-$PMANa_{615}$ in higher q region, representing the core of the micelle,

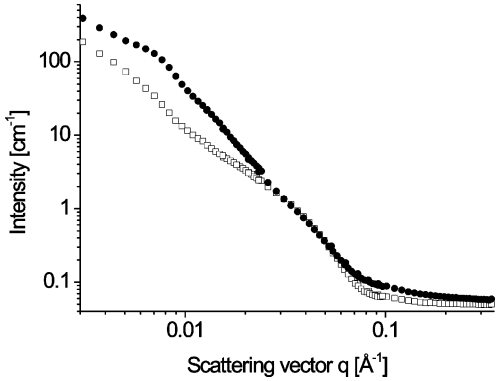

Figure 6. SANS curves of PIB_{75}-*b*-$PMANa_{615}$ micelles (□) and their IPECs prepared at $Z = 0.4$ (●), $c_{TRIS} = 0.01$ M, $\alpha = 1$, $c_{NaCl} = 0.1$ M.

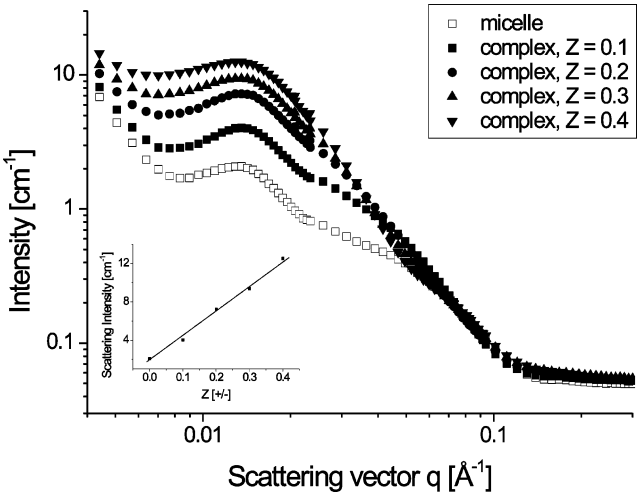

Figure 7. SANS curves of PIB_{20}-*b*-$PMANa_{100}$ micelles, $\alpha = 1.0$, (□) and of their IPECs prepared at (from bottom to top) $Z = 0.1$, 0.2, 0.3, and 0.4, $c_{TRIS} = 0.01$ M, $c_{NaCl} = 0.1$ M. Inset: Dependence of scattering intensity at $q = 0.0136$ Å^{-1} on *Z*.

show almost the same shape. Only at lower *q* values, i.e., larger dimensions, an increase in scattering intensity can be observed. This is a clear sign for higher M_w of the micelle after interacting with P4VPQ, proving complexation of the positively charged P4VPQ with the carboxylic groups of the PMAA. This is similarly observed for the other samples.

The increase of the scattering intensity can also be seen upon increasing content of the cationic polyelectrolyte by stepwise addition to the micellar solutions (Figure 7).

The more P4VPQ is added, the higher is the total scattering intensity. Again, in the higher *q*-region, the change of the curves is not that pronounced, showing almost no effect of complexation on the core of the micelle. When plotting the scattering intensity at the peak maximum ($q = 0.0136$ Å) against the *Z*-value, a linear dependence is observed (inset in Figure 7). Additionally, the position of the peak maximum does not change. This is a clear indication that the number density of complex micelles stays constant. Hence the aggregation number remains unchanged, even if *Z* changes from 0 up to 0.4.

In our previous work[25] we reported on the dynamic behavior of the micelles formed by the PIB_x-*b*-$PMAA_y$ copolymer in aqueous solutions, i.e., the aggregation number, N_{agg} was found to be sensitive to variations of external stimuli. In Figure 8 similar experiments were carried out for IPECs formed by PIB_{30}-*b*-$PMAA_{190}$, complexed with P4VPQ, $Z = 0.4$ at $c_{NaCl} = 0.1$ M. In these experiments, the scattering curves obtained from complex

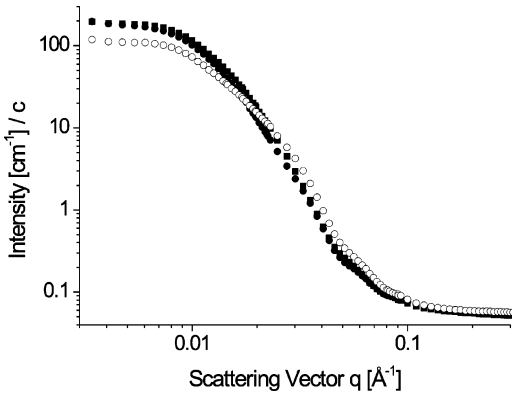

Figure 8. SANS curves of PIB_{30}-*b*-$PMANa_{190}$ micellar solutions complexed with P4VPQ, $Z = 0.4$, $c_{NaCl} = 0.1$ M, directly prepared at pH 10 (○) and 7 (black square) and a sample prepared at pH 11.5 and brought to pH 7 (●).

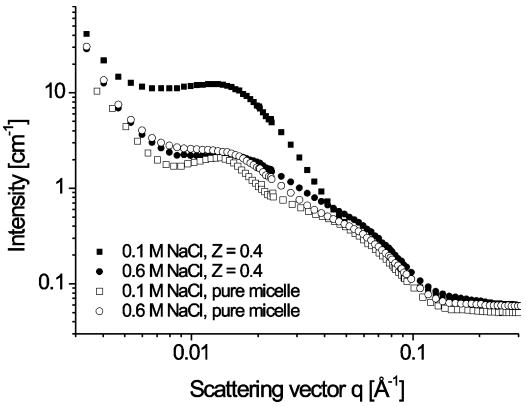

Figure 9. Dissociation of complex formed by PIB_{20}-*b*-$PMAA_{100}$ with P4VPQ, $Z = 0.4$, $c_{TRIS} = 0.01$ M. The SANS scattering curves represent (from top to bottom, full symbols) $c_{NaCl} = 0.1$ and 0.6 M. The open symbols represent (from top to bottom) the scattering curves obtained by micellar solutions of PIB_{20}-*b*-$PMAA_{100}$, $c_{NaCl} =$ 0.1 and 0.6 M, $c_{TRIS} = 0.01$ M.

solutions directly prepared at pH 10 and 7, respectively, were compared to the scattering coming from a solution prepared at pH 11.5 and, after some days of equilibration, brought to pH 7. From Figure 8 it can be clearly seen that the scattering behavior for the two samples at pH 7, which were prepared in a different way, coincides. The most important point is that the scattering curves in the range where the scattering coming from the PIB core is monitored superimpose. Thus, it can be concluded that the core size of the two differently prepared samples is similar, whereas the scattering curve for the sample at pH 10 is clearly different.

3.2. Salt-Induced Dissociation of Complexes. *3.2.1. SANS.* An interesting aspect of the complexes is their ability to respond on external stimuli, namely changes in ionic strength. In this work, we increased the ionic strength of our complex solutions up to $c_{NaCl} = 0.6$ M. In Figure 9 SANS curves of samples with a selection of different salt contents are shown. The complexes consists of PIB_{20}-*b*-$PMAA_{100}$ micelles and P4VPQ with a $\overline{DP_w}$ of 500. The *Z* value is set to 0.4, meaning that 40% of the negative charges on the PMAA chains are complexed. The salt concentration is increased from 0.1 to 0.6 M NaCl (full symbols). The scattering curves represented by the open symbols correspond to solutions of the pure PIB_{20}-*b*-$PMANa_{100}$ micelles at 0.1 (open squares) and 0.6 M NaCl (open circles), respectively.

The most important change of the curves is the decrease of the scattering intensity in the intermediate *q* range (0.01−0.03 Å^{-1}). This correlation peak can be attributed to interactions

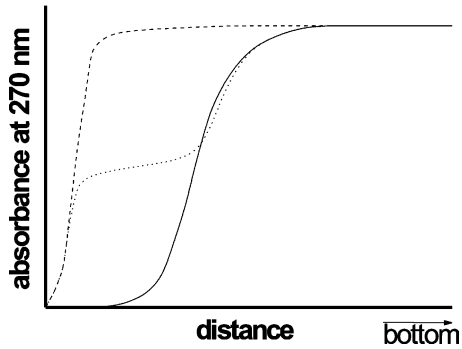

Figure 10. Typical sedimentation patterns (scan mode, detection at $\lambda = 270$ nm) for the aqueous mixtures of complexes of PIB_{20}-*b*-$PMAA_{100}$ micelles and P4VPQ at $Z = 0.4$ obtained at $c_{NaCl} = 0.1$ (line) and 0.4 M NaCl (dotted), $c_{TRIS} = 0.01$ M and pure P4VPQ (dashed).

between complexes. The decrease in scattering intensity can be seen in the low q region. As the scattering intensity is directly proportional to the molecular weight of the scattering particle, the $\overline{M_w}$ of the complexes apparently decreases. The contribution of the free P4VPQ can be neglected to a first approximation, as the scattering intensity is far below the scattering coming from the pure micelles.

Another indication on changes in the superstructure is the slight shift of the peak maximum of the correlation peak in Figure 9. The movement from $q = 0.0135$ Å^{-1} (0.1 M NaCl) to $q = 0.0105$ Å^{-1} (0.3 M NaCl, not shown here) back to $q = 0.0132$ Å^{-1} represents a change in distance of the scattering centers from 46.5 to 59.8 and 48.6 nm, respectively. Thus, the average distance between the scattering centers increases slightly, seen by a shift of the correlation peak.

Gohy et al.[17] also reported on water-soluble complexes formed by sodium poly(4-styrenesulfonate) (PSS) and poly(2-vinylpyridinium)-*b*-poly(ethylene oxide) (P2VP-*b*-PEO). They observed monodisperse spherical micelles, their stability depending on the pH and ionic strength. The complexes dissociate above a critical salt concentration, seen by a decrease in scattering intensity of the solutions. Thus, they conclude that the micelles with the complex core are dissolved. Kabanov et al.[32] reported on changes of structures of complexes consisting of poly(acrylic acid) (PAA) and poly(ethylene imine) (PEI) with increasing salt concentration. They investigated their behavior in aqueous media with low ionic strength, as well as in an intermediate region. Here they observed a rearrangement of the charged chains. The dissociation of the complex was reported to occur at high salt concentrations, resulting in separated polyelectrolytes.

3.2.2. Analytical Ultracentrifugation. Figure 10 shows typical sedimentation patterns obtained in the scan mode for solutions of IPECs based on PIB_{20}-*b*-$PMAA_{100}$ micelles at relatively low (line) and high (dotted) concentration of NaCl, i.e., at 0.1 and 0.4 M NaCl, respectively. As is seen, only one type of the sedimenting particles (one step in Figure 10) with sedimentation coefficient ($S \approx 25$ Sv) considerably exceeding that of the free cationic macromolecules ($S \approx 1.5-2$ Sv; sedimentation pattern is given in Figure 10 by a dashed line) is observed at 0.1 M NaCl. These species sedimenting with rather high sedimentation velocity represent particles of micellar interpolyelectrolyte complex. At the same time, two types of sedimenting particles (two steps in Figure 10, dotted) with markedly different sedimentation coefficients of ca. 1.5 and ca. 23 Sv are clearly detected at 0.4 M NaCl. The species with low sedimentation coefficient are

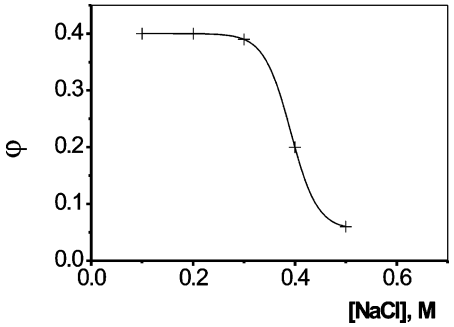

Figure 11. Dependence of the stoichiometry of IPEC species of PIB_{20}-*b*-$PMAA_{100}$ at $Z = 0.4$ on the concentration of NaCl; $c_{TRIS} = 0.01$ M.

assigned to free cationic macromolecules, while those with high sedimentation coefficient are considered to be particles of micellar interpolyelectrolyte complex. At relatively high concentrations of NaCl, therefore, free cationic macromolecules appear to release from the complex species, thus coexisting with them. The relative height of the first step in the sedimentation pattern shown in Figure 10 represents a fraction, f, of free cationic macromolecules. They behave similarly as the complexes of poly(methacrylic acid) and P4VPQ, reported by Pergushov et al.[33]

The stoichiometry of the complex species, φ, defined as a ratio of the pyridinium groups to carboxylate groups incorporated in the IPEC can be calculated according to eq 1

$$\varphi = Z(1 - f) \tag{1}$$

Figure 11 demonstrates the dependence of φ on the concentration of NaCl in the aqueous mixtures of PIB_{20}-*b*-$PMAA_{100}$ micelles and P4VPQ. For $c_{NaCl} < 0.3$ M, the values of φ remain constant and coincide with Z, while for $c_{NaCl} \geq 0.3$ M, φ gradually decreases with increasing ionic strength, approaching finally a value of $\varphi \approx 0$ at $c_{NaCl} \approx 0.6$ M. This finding undoubtedly indicates that IPECs undergo complete dissociation to their polymeric constituents, that is, PIB_{20}-*b*-$PMAA_{100}$ micelles and P4VPQ, at relatively high ionic strength. The obvious reason for that is the effective screening of the electrostatic interaction between PMAA blocks and P4VPQ chains by small ions, which increase the relative solubility of the P4VPQ in the solvent.

3.2.3. Titrations. The dissociation of the complex can also be seen from potentiometric titrations of complexes with NaCl solutions. The activity of the Na^+ ions was monitored with a Na^+-selective electrode. Relative to the background curve (pure NaCl), an increase of the signal can be observed (not shown here). However, in the intermediate range at a salt concentration of 0.5 M NaCl a small bump can be detected. This is obvious in Figure 12. Here, a curve representing a difference between the complex solution and the background is depicted. The main reason that the complex shows a higher activity compared to the background solution is the fact that NaCl is produced during the neutralization of the polyacid. The amount of the NaCl is around $n_{NaCl} = 2.3\ 10^{-4}$ mol. In the graph shown, two distinct regions can be seen. The first maximum in the relative response occurs at a salt concentration of 0.23 M. Starting from this point, the slope of the titration curve of the complex is smaller than the slope of the background measurement. This results in a decrease of the differential signal seen in the graph.

This phenomenon can be explained by the activity of Na^+ ions in both solutions. The rate of addition of the brine solution was the same in both cases. Hence, the overall amount of Na^+ ions

(32) Kabanov, V. A.; Zezin, A. B. *Pure Appl. Chem.* **1984**, *56*, 343.

(33) Pergushov, D. V.; Izumrudov, V. A.; Zezin, A. B.; Kabanov, V. A. *Pol. Sci. A* **1995**, *37*, 1081.

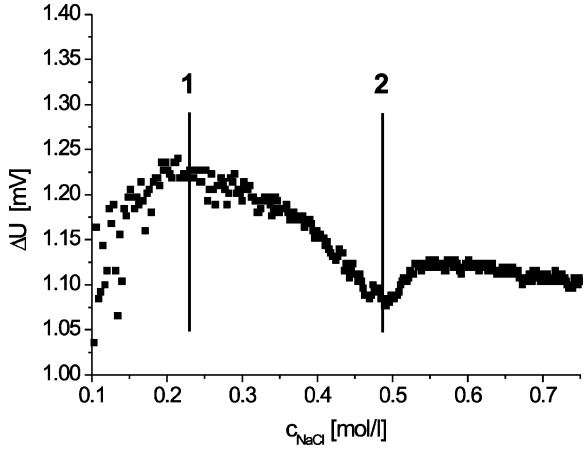

Figure 12. Difference of potentiometric titration (voltage U) curves of mixtures of PIB_{75}-*b*-$PMAA_{1600}$ and P4VPQ ($Z = 0.4$) depending on the concentration of NaCl with a sodium-selective electrode. A relative maximum (1) and a minimum (2) of the difference is observed.

in the solution is the same. The only difference is their contribution to the activity. In the reference solution, all sodium ions are measured. In the case of the complex, at the beginning of the titration, all sodium ions contribute to the activity of the solution. Starting from a certain point (1), the complex slowly starts dissociating upon addition of further salt. Thus, the additional negative charges of the PMAA chains are able to condense Na^+ ions. Once trapped by the micellar corona, the sodium ions do not contribute to the Na^+ activity in the solution any more. Hence, compared to the background measurement, the relative activity of the sodium ions decreases.

This effect remains until a minimum of the curve (2) is reached. Starting from this point, the curve slightly increases until a plateau is reached. The minimum at a salt concentration of $c_{NaCl} = 0.49$ M can be explained by the end of dissociation of the complex. Any further Na^+ ion added to the solution of the complex now contributes to the activity of the solution in the same way as for the background solution. The slight increase of the curve is related to the fact that the PIB_x-*b*-$PMAA_y$ micelles also react on changes in ionic strength of the solvent.[25] The increased screening effect of the charges along the PMAA chains due to Manning condensation enabling the arms to arrange more densely. Therefore, solvent also containing sodium ions is expelled from the corona. Hence, the Na^+ ions are again detectable by the Na-selective electrode and contribute to the activity of the solution. The same behavior can be observed for all measured complexes (Figure 13).

The values obtained by titration nicely agree with the results obtained from SANS data (Figure 9). In Table 3 a comparison of the starting points and the end of the dissociation process of the complexes is shown. From SANS data, a start of dissociation above a salt concentration of beyond 0.2 M can be observed as well. Above a salt concentration of 0.5 M, no noticeable change in the scattering behavior can be observed. This is another indication that the dissociation of the complexes takes place between 0.2 and 0.5 M salt content of the complex solution.

As already reported by Kabanov et al.,[32] the driving force for the formation of complexes is the release of counterions of the polyelectrolyte species. This leads to an increase in entropy of the whole system. In complex particles, the counterions are replaced by an oppositely charged polyelectrolyte. The released counterions are contributing to the activity of the ions present in the solution. During the process of dissociation of the complex,

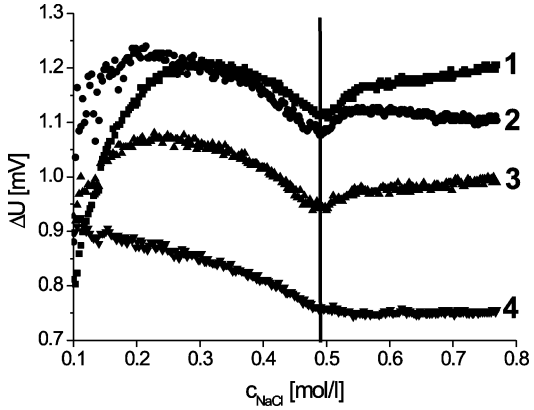

Figure 13. Difference of titration curves with sodium-selective electrode for complexes formed with PIB_{75}-*b*-$PMAA_{615}$ (1), PIB_{75}-*b*-$PMAA_{1600}$ (2), PIB_{25}-*b*-$PMAA_{325}$ (3), and PIB_{30}-*b*-$PMAA_{190}$ (4), $Z = 0.4$.

Table 3. Comparison of the Different Stages of the Dissociation Process of the Complex Formed by Different PIB_x-*b*-$PMAA_y$ Diblock Copolymers by Means of SANS and Potentiometric Titration

PIB_x-*b*-$PMAA_y$	titration start diss. c_{NaCl} [M]	titration end diss. c_{NaCl} [M]	SANS start diss. c_{NaCl} [M]	SANS end diss. c_{NaCl} [M]
75−1600	0.23	0.49	−	−
75−615	0.30	0.50	−	−
25−325	0.27	0.50	−	−
30−190	-	0.49	−	−
20−100	−	−	>0.2; <0.3	>0.4; ≈0.5

the counterions, according to Manning,[34] should be partially condensed on the polyelectrolyte chains. For polyelectrolyte brushes and stars, the fraction of condensed counterions has been found to be >90%.[35,36]

4. Conclusion

In this paper a detailed investigation of the formation, structure, and dissociation of IPECs formed by PIB_x-*b*-$PMAA_y$ with P4VPQ is presented. PIB_x-*b*-$PMAA_y$ diblock copolymers with a large variation of $\overline{DP_n}$ of both hydrophobic PIB and hydrophilic PMAA blocks are used to form water-soluble complexes with core−shell−corona structure. From cryo-TEM images, a spherical shape of the IPECs can be concluded.

The process of formation of complexes can be subdivided in a kinetically driven and a thermodynamically driven process. Upon addition of the polycation solution to the micellar PIB_x-*b*-$PMAA_y$ solution, first an increase in turbidity of the solution can be observed. In this kinetically driven regime, large assemblies of micelles are formed. With time, these aggregates are equilibrating toward the thermodynamically more stable species of a single micelle with a complex shell formed around the hydrophobic PIB core. The formation process can also be seen by means of SANS, leading to higher scattering intensity with increasing *Z*. By means of SANS, it was shown that the complexes formed remain dynamic with respect to external stimuli as pH jumps, as already reported for the pure micellar system.[25]

SANS was also used to follow the salt-induced dissociation of the complex. Increasing the ionic strength of the IPEC solution leads to a release of the polycation, starting from about 0.2 M

(34) Ray, J.; Manning, G. S. *Macromolecules* **1999**, *32*, 4588.
(35) Das, B.; Guo, X.; Ballauff, M. *Prog. Colloid Polym. Sci.* **2002**, *121*, 34.
(36) Plamper, F. A.; Schmalz, A.; Penott-Chang, E.; Drechsler, M.; Jusufi, A.; Ballauff, M.; Müller, A. H. E. *Macromolecules* **2007**, *40*, 5689.

NaCl. Beyond 0.5 M NaCl, almost no difference in scattering behavior of the IPEC solution compared to pure micellar solution can be stated. This strongly suggests a total dissociation of the IPEC. By means of titration with a sodium-selective electrode, the decrease of the activity of the Na^+ ions can be explained by substitution of the polycation due to Manning condensation. After complete dissociation of the IPEC, the activity of the IPEC solution, upon addition of further NaCl, follows the behavior of a background solution.

Comparing different techniques, a starting point of the complex dissociation at an ionic strength of about 0.2 M can be concluded. Independent on the block lengths of both PIB and PMAA the IPEC is completely dissociated at $c_{NaCl} \approx 0.5$ M.

Acknowledgment. This work was supported by the European Union within the Marie Curie RTN Polyamphi and by DFG within the ESF EUROCORES Programme SONS. ILL is gratefully acknowledged for providing SANS beam time and travel support. D.V.P. thanks DFG for the financial support of his research stays at the Universität Bayreuth.

LA701835R